HHS Public Access

Author manuscript

Science. Author manuscript; available in PMC 2018 November 02.

Published in final edited form as:

Science. 2017 September 29; 357(6358): 1406–1411. doi:10.1126/science.aan4994.

Gating of social reward by oxytocin in the ventral tegmental area

Lin W. Hung[1,2], **Sophie Neuner**[#1], **Jai S. Polepalli**[#1], **Kevin T. Beier**[#1,3,4], **Matthew Wright**[3,5], **Jessica J. Walsh**[1], **Eastman M. Lewis**[6], **Liqun Luo**[3,4], **Karl Deisseroth**[3,5], **Gül Dölen**[6], and **Robert C. Malenka**[1,†]

[1]Nancy Pritzker Laboratory, Department of Psychiatry and Behavioral Sciences, Stanford University, Stanford, CA, USA.

[2]The Florey Institute of Neuroscience and Mental Health, Parkville, Victoria, Australia.

[3]Howard Hughes Medical Institute, Stanford University, Stanford, CA, USA.

[4]Department of Biology, Stanford University, Stanford, CA, USA.

[5]Departments of Bioengineering and Psychiatry and Behavioral Sciences, Stanford University, Stanford, CA, USA.

[6]Department of Neuroscience, John Hopkins University, Baltimore, MD, USA.

[#] These authors contributed equally to this work.

Abstract

The reward generated by social interactions is critical for promoting prosocial behaviors. Here we present evidence that oxytocin (OXT) release in the ventral tegmental area (VTA), a key node of the brain's reward circuitry, is necessary to elicit social reward. During social interactions, activity in paraventricular nucleus (PVN) OXTneurons increased. Direct activation of these neurons in the PVN or their terminals in the VTA enhanced prosocial behaviors. Conversely, inhibition of PVN OXTaxon terminals in the VTA decreased social interactions. OXT increased excitatory drive onto reward-specific VTA dopamine (DA) neurons. These results demonstrate that OXTpromotes prosocial behavior through direct effects on VTA DA neurons, thus providing mechanistic insight into how social interactions can generate rewarding experiences.

Positive prosocial experiences are critical for cooperative and productive interactions between members of a group. Conversely, the inability to experience reinforcement from social interactions (henceforth, "social reward") is a symptom of neuropsychiatric disorders, notably autism (1). Over the past decade, evidence has accumulated that the neuropeptide oxytocin (OXT) plays a critical role in social behaviors and may have therapeutic utility for the treatment of social behavior deficits (2). An important clue that OXT exerts some of its actions by influencing the brain's reward circuitry came from work demonstrating that OXT

[†]Corresponding author. malenka@stanford.edu.

SUPPLEMENTARY MATERIALS

www.sciencemag.org/content/357/6358/1406/suppl/DC1

Materials and Methods

Figs. S1 to S11

References (28–38)

receptors (OXTrs) in the nucleus accumbens (NAc) of prairie voles were critical for pair bonding (3). Subsequent work suggested that OXT action in the NAc is also important for social reward in mice (4). OXT action in the ventral tegmental area (VTA), another key node of reward circuitry, may also be critical for regulating social interaction cues (5, 6) and social reward (7). Although social interactions in mice are accompanied by increases in activity in NAc-projecting VTA dopamine (DA) neurons (8), which are critical for motivated behaviors (9), the mechanism by which VTA DA neuron activity is gated during social behaviors is unknown.

Rabies virus–based tracing methods have suggested that OXT neurons in the paraventricular nucleus (PVN) send axonal projections to the VTA (10). To visualize these OXTergic projections directly, we injected AAV_{DJ}-DIO-eGFP (adeno-associated virus DJ with double-floxed inverse open reading frame flanking enhanced green fluorescent protein) into the PVN of a knock-in mouse line expressing Cre recombinase in OXT neurons (*OXTiresCre*) (Fig. 1A). Consistent with previous reports (11), we found colocalization of eGFP and OXT immunostaining in the PVN, with no detectable eGFP expression in vasopressin (AVP) PVN neurons (~48% of OXT neurons expressed eGFP in tissue sections from eight animals) (Fig. 1B). Axons expressing eGFP were present in the VTA (Fig. 1B), often in close proximity to OXTr-expressing DA neurons (Fig. 1C), which were localized using an OXTr-Venus knock-in mouse line (12). Tail-vein fluorogold injections revealed that both magnocellular and parvocellular PVN OXT neurons projected to the VTA (fig. S1).

To investigate whether PVN neurons projecting to the VTA are necessary for social reward, we inhibited these neurons by injecting a retrogradely transported canine adenovirus expressing Cre (CAV2-Cre) into the VTA and an AAV expressing a Cre-dependent inward rectifying potassium channel (AAV_{DJ}-DIO-Kir2.1-ZsGreen) into the PVN (Fig. 1D and fig. S2A). Two weeks after viral injections, mice were subjected to a social conditioned place preference (CPP) assay (4). Mice expressing the potassium channel (Kir2.1) in VTA-projecting PVN neurons exhibited reduced preference for the socially conditioned context (Fig. 1, F and G) compared with control mice expressing ZsGreen (Fig. 1, E and G). Expression of Kir2.1 in VTA-projecting PVN neurons did not influence the CPP generated by administration of cocaine (fig. S2, B to D) or locomotor activity (fig. S2E).

To test whether OXT action in the VTA is necessary for social reward, we selectively ablated OXTrs in the VTA by injecting an AAV_{DJ}-Cre-eGFP into the VTA of floxed OXTr (*OXTr*$^{fl/fl}$) mice (Fig. 1H) (13). Unlike wild-type mice injected with the same virus, mice lacking OXTrs in the VTA exhibited no social CPP (Fig. 1, I to K). To determine whether OXTrs specifically in DA neurons are necessary for social reward, we crossed *OXTr*$^{fl/fl}$ mice with *DATCre* mice (14) (Fig. 1L; fig. S3 illustrates the breeding strategy). Homozygous OXTr DA knockout (KO) mice exhibited no social CPP, whereas littermate control mice expressed normal social CPP, as did heterozygous OXTr DA KO mice (Fig. 1, M to O, and fig. S4, A to C). Deleting OXTrs from sub-populations of GABAergic cells by crossing *OXTr*$^{fl/fl}$ mice with *GAD2Cre* mice (Fig. 1P) had no effect on social CPP (Fig. 1, Q to S). All of these mouse lines exhibited CPP in response to cocaine and normal locomotor activity in the open field after saline and cocaine injections (fig. S4, D to K).

To determine whether activity in VTA-projecting PVN neurons increases during social interactions, we injected CAV2-Cre into the VTA of Ai14 tdTomato reporter mice to label cells projecting to the VTA (Fig. 2A) and assessed the expression of the immediate early gene *c-fos* (15). After social interaction, the proportion of VTA-projecting PVN neurons expressing *c-fos* tripled compared with that in mice that interacted with a toy mouse (Fig. 2B). To more directly measure PVN OXT neuronal activity during social interactions, we targeted the fluorescent calcium indicator GCaMP6m to PVN OXT neurons by injecting AAV_{DJ}-DIO-GCaMP6m into the PVN of *OXTiresCre* mice and performed fiber photometry (Fig. 2, C to E). No increase in fluorescent signal occurred when these mice interacted with a toy mouse (Fig. 2F). However, there was a time-locked increase in the activity of PVN OXT neurons during socialcontact witha juvenile (Fig. 2, G and H).

We next investigated whether optogenetic activation of PVN OXT neurons alone is rewarding by injecting a Cre-dependent AAV expressing ChETA (AAV_{DJ}-DIO-ChETA-eYFP) into the PVN of *OXTiresCre* mice and implanting optical fibers in the PVN (ChETA, channelrhodopsin-2 with threo-nine substituted for glutamic acid at position 123; eYFP, enhanced yellow fluorescent protein) (Fig. 2, I and J). *OXTiresCre* mice injected with AAV_{DJ}-DIO-eYFP served as controls. Consistent with previous results (16), optogenetic activation of PVN OXT neurons did not reinforce operant behaviors, as assayed using real-time CPP (RT-CPP) (Fig. 2K and fig. S5, A and B) and nose-poking for intracranial self-stimulation (ICSS) (Fig. 2L and fig. S5, C to G).

Because PVN OXT neuron activity appears to be important for social reward, yet their activation alone did not drive instrumental learning, we hypothesized that activation of these neurons in a social context would facilitate this type of learning. In a social RT-CPP (sRT-CPP) protocol, mice were exposed to a confined novel juvenile mouse on day 1 without any stimulation (Fig. 2M). On day 2, optogenetic stimulation occurred when mice entered the compartment containing the confined familiar juvenile. In *OXTiresCre* mice expressing eYFP in PVN OXT neurons, photostimulation did not cause an increase in preference for the social context on day 2, whereas the same photostimulation in mice expressing ChETA elicited a clear increase in preference for the social context (Fig. 2, N to P, and fig. S5, H to J). Locomotion during these assays was not affected (fig. S5K).

OXT has been implicated in social memory and learning, and because mice prefer interacting with a novel conspecific over a familiar one (17), it is possible that PVN OXT neuron activation interfered with the memory of the day 1 interaction, thus making the familiar juvenile mouse appear novel on day 2. We therefore performed a three-chamber sociability task during which photostimulation of PVN OXT neurons was applied continuously while mice could freely explore compartments with an empty vessel or a vessel containing a novel juvenile (fig. S6, A to C). Immediately after this session, a novel juvenile was placed in the previously empty vessel (fig. S6D). Mice expressing ChETA in PVN OXT neurons explored the compartment containing the novel juvenile in a similar manner to that of control mice expressing eYFP; both sets of mice spent more time exploring the novel juvenile (fig. S6E).

To test whether stimulating OXT release specifically in the VTA could replicate the behavioral results of PVN OXT neuron soma stimulation, we expressed ChETA or eYFP in PVN OXT neurons in *OXTiresCre* mice and implanted optical fibers in the VTA (Fig. 3A and fig. S7, A and B). Stimulation of PVN OXT neuron axons in the VTA replicated all of the results generated by soma stimulation. Neither RT-CPP nor ICSS was elicited (fig. S7, C to H); however, clear sRT-CPP was elicited in ChETA-expressing mice but not in control eYFP-expressing mice (Fig. 3, B and C, and fig. S7, I and J). Administration of an OXTr antagonist (L-368,899 HCl; 5 mg per kilogram of body weight, injected intraperitoneally) prevented the sRT-CPP elicited by stimulation of PVN OXT neuron terminals in the VTA (Fig. 3, D and E, and fig. S7, K and L) but had no detectable effects on its own (fig. S7M).

To further explore whether activating PVN OXT neuron axons in the VTA enhances sociability, we performed a juvenile interaction assay using different photostimulation protocols (fig. S8A). Photostimulation only when mice were in social contact (proximity <2 cm) over 3 days caused an increase in the time spent interacting, compared with that observed for eYFP-expressing control mice receiving the same stimulation (Fig. 3, F and G). In contrast, photostimulation throughout the duration of the experiment had no effect (Fig. 3, H and I). Furthermore, applying the same protocols but with a toy mouse had no effect on toy mouse interaction times (fig. S8, B to F).

These experiments provide evidence that activation of PVN OXT neuron axons in the VTA promotes sociability but do not prove that OXT release in the VTA normally contributes to such behaviors. We therefore repeated our assays in *OXTiresCre* mice expressing the inhibitory opsin NpHR3.0 in a Cre-dependent manner (AAV_{DJ}-DIO-NpHR3.0-eYFP) in the PVN, with optical fibers implanted in the VTA (Fig. 3J). Inhibiting PVN OXT neuron projections in the VTA reduced the preference for the social context (Fig. 3, K to N), whereas the same stimulation did not have effects during standard RT-CPP assays (fig. S9, A and B). Similarly, inhibiting PVN OXT projections in the VTA through NpHR3.0 activation reduced the time spent interacting with a novel juvenile over the course of 3 days when applied in a context-dependent manner (Fig. 3, O and P) but not when stimulation was applied continuously during the experiment (Fig. 3, Q and R).

A simple hypothesis to explain the behavioral results is that OXT release in the VTA occurs early in the time course of a social interaction and enhances the excitability of DA neurons projecting to the NAc. This increases DA release in the NAc, which reinforces the social interaction. We crossed *DATCre* mice with Ai14 mice to label DA cells with tdTomato, injected fluorescent retrobeads into the NAc medial shell (NacMedS), and made recordings from NAcMedS-projecting VTA DA neurons (Fig. 4, A and B), activity in which increases during social interactions (8). In cell-attached current clamp recordings, application of the OXTr agonist [Thr^4,Gly^7]-oxytocin (TGOT; 1 μM) increased spontaneous spiking in DA neurons, an effect reversed by application of the OXTr antagonist L-368,899 HCl (1 μM; Fig. 4, C and D). DA cells that did not contain retrobeads and presumably do not project to the NAcMedS did not exhibit a change in spiking in response to TGOT (Fig. 4, C and D).

The number of spikes elicited by depolarizing current pulses in NAcMedS-projecting DA neurons did not change during TGOT application (fig. S10, A and B), nor did the cells'

resting membrane potential and input resistance (fig. S10, C and D). However, TGOT increased evoked excitatory post-synaptic current (EPSC) amplitude when DA cells were voltage-clamped at −60 mV and simultaneously decreased evoked inhibitory postsynaptic current (IPSC) amplitude when the same cells were voltage-clamped at 0 mV (Fig. 4, E and F). These synaptic effects of TGOT were reversed by application of the OXTr antagonist (Fig. 4, E and F). The decrease in IPSC amplitude was associated with an increase in the IPSC paired pulse ratio (PPR), whereas EPSC PPRs were not affected by TGOT (Fig. 4G), suggesting that OXT acts presynaptically at inhibitory synapses and post-synaptically at excitatory synapses. Consistent with these sites of OXT action in the VTA, when recordings were made from NAcMedS-projecting DA neurons lacking OXTrs (i.e., in slices from the cross of $OXTr^{fl/fl}$ and Ai14:DATcre mice), TGOT caused no changes in EPSCs but evoked a decrease in IPSC amplitude and an increase in IPSC PPRs (Fig. 4, H to J). These results from acute slices are consistent with in vivo studies demonstrating that optogenetic stimulation of PVN OXT neurons increased the proportion of *c-fos*–positive VTA DA neurons in the anatomical regions where NAcMedS-projecting DA neurons are located (fig. S11, A to D).

We have provided evidence that OXT release in the VTA enhances the activity of a specific population of DA neurons that influence social interactions (8). Several results indicate that this action of OXT is important for the reinforcing component of social interactions. First, inhibition of OXT action in the VTA—by inhibiting the activity of VTA-projecting PVN neurons or genetically deleting OXTrs from VTA DA neurons—prevented social CPP. Second, the activity of PVN OXT neurons increased during social interactions. Third, optogenetic activation of PVN OXT neuron inputs in the VTA enhanced sociability, but only when activation of OXT axons occurred approximately during social interactions. Fourth, optogenetic inhibition of the OXT inputs in the VTA reduced sociability.

OXT is important for a range of behaviors in rodents owing to its specific actions in a variety of brain structures (18–22), including the VTA (7). Our results provide mechanistic insights into how OXT can modulate activity in the VTA, which we demonstrate is critical for mediating some of OXT's effects on sociability. Peripheral OXT administration may enhance human VTA blood oxygen level–dependent activity in functional magnetic resonance imaging studies (23, 24), suggesting that our findings have relevance for understanding OXT actions in the human brain. However, the clinical utility of OXT administration for treating social deficits in patients with neuro-psychiatric disorders remains unclear (2), even though OXT treatment can ameliorate social behavior deficits in mouse models of autism (5, 25). Elucidating the circuit-specific mechanisms by which OXT contributes to social reward is a critical step in bridging the translational gap between animal and human work (26) and may eventually lead to the development of novel therapies for social behavior deficits.

Note added in proof: In agreement with one major conclusion of our work, a recent publication (27) reports that OXT release enhances the activity of VTA DA neurons.

Supplementary Material

Refer to Web version on PubMed Central for supplementary material.

ACKNOWLEDGMENTS

This work was supported by a grant from the Simons Foundation Autism Research Initiative (to R.C.M.). G.D. was supported by the Hartwell Foundation, Kinship Foundation, and Klingenstein-Simons Foundation. All data are reported in the main text and supplementary materials, stored at Stanford, and available upon reasonable request.

REFERENCES AND NOTES

1. Chevallier C, Kohls G, Troiani V, Brodkin ES, Schultz RT, Trends Cogn. Sci 16, 231–239 (2012). [PubMed: 22425667]
2. Young LJ, Barrett CE, Science 347, 825–826 (2015). [PubMed: 25700501]
3. Young LJ, Wang Z, Nat. Neurosci 7, 1048–1054 (2004). [PubMed: 15452576]
4. Dölen G, Darvishzadeh A, Huang KW, Malenka RC, Nature 501, 179–184 (2013). [PubMed: 24025838]
5. Buffington SA et al., Cell 165, 1762–1775 (2016). [PubMed: 27315483]
6. Shamay-Tsoory SG, Abu-Akel A, Biol. Psychiatry 79, 194–202 (2016). [PubMed: 26321019]
7. Song Z et al., Psychoneuroendocrinology 74, 164–172 (2016). [PubMed: 27632574]
8. Gunaydin LA et al., Cell 157, 1535–1551 (2014). [PubMed: 24949967]
9. Lammel S, Lim BK, Malenka RC, Neuropharmacology 76, 351–359 (2014). [PubMed: 23578393]
10. Beier KT et al., Cell 162, 622–634 (2015). [PubMed: 26232228]
11. Wu Z et al., PLOS ONE 7, e45167 (2012). [PubMed: 23028821]
12. Yoshida M et al., J. Neurosci 29, 2259–2271 (2009). [PubMed: 19228979]
13. Lee HJ, Caldwell HK, Macbeth AH, Tolu SG,Young WS, 3rd, Endocrinology 149, 3256–3263 (2008). [PubMed: 18356275]
14. Lammel S et al., Neuron 85, 429–438 (2015). [PubMed: 25611513]
15. Schilling K, Luk D, Morgan JI, Curran T, Proc. Natl. Acad. Sci. U.S.A 88, 5665–5669 (1991). [PubMed: 1648227]
16. Choe HK et al., Neuron 87, 152–163 (2015). [PubMed: 26139372]
17. Ferguson JN et al., Nat. Genet 25, 284–288 (2000). [PubMed: 10888874]
18. Burkett JP et al., Science 351, 375–378 (2016). [PubMed: 26798013]
19. Knobloch HS et al., Neuron 73, 553–566 (2012). [PubMed: 22325206]
20. Marlin J, Mitre M, D'amour JA, Chao MV, Froemke RC, Nature 520, 499–504 (2015). [PubMed: 25874674]
21. Oettl LL et al., Neuron 90, 609–621 (2016). [PubMed: 27112498]
22. Owen SF et al., Nature 500, 458–462 (2013). [PubMed: 23913275]
23. Groppe SE et al., Biol. Psychiatry 74, 172–179 (2013). [PubMed: 23419544]
24. Paloyelis Y et al., Biol. Psychiatry 79, 693–705 (2016). [PubMed: 25499958]
25. Peñagarikano O et al., Sci. Transl. Med 7, 271ra8 (2015).
26. Nestler EJ, Hyman SE, Nat. Neurosci 13, 1161–1169 (2010). [PubMed: 20877280]
27. Xiao L, Priest MF, Nasenbeny J, Lu T, Kozorovitskiy Y, Neuron 95, 368–384.e5 (2017). [PubMed: 28669546]

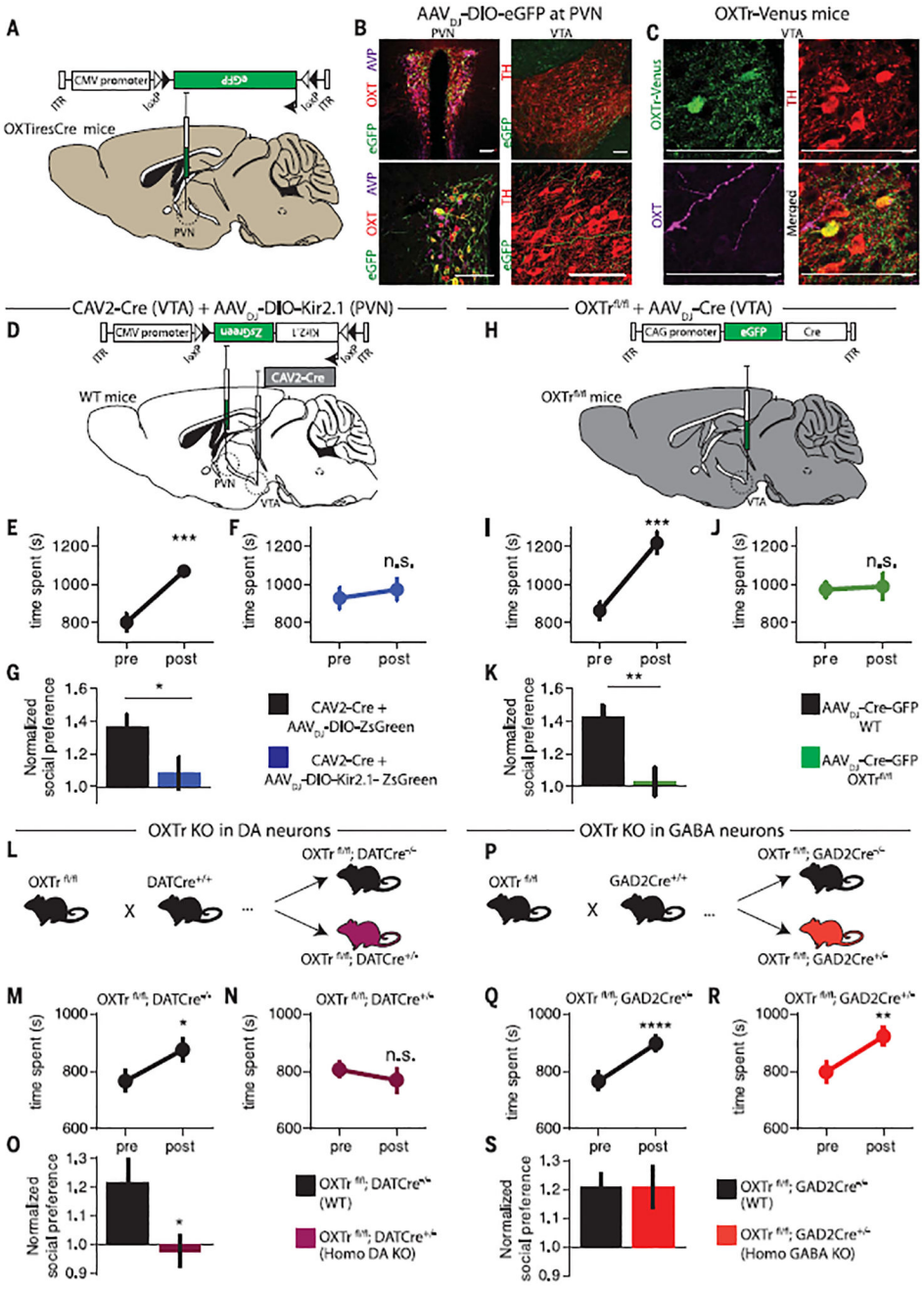

Fig. 1. PVN OXT projections to VTA DA neurons are required for social reward.

(**A**) AAV$_{DJ}$-DIO-eGFP was injected into the PVN of OXTiresCre mice to label OXTneurons. ITR, inverted terminal repeats; CMV, cytomegalovirus. (**B**) Immunostaining showing (left) colocalization of eGFP (green) with OXT (red) but not AVP (magenta) in PVN neurons and (right) eGFP fibers (green) adjacent to DA neurons (red) in the VTA.TH, tyrosine hydroxylase. Scale bars, 100 μm. (**C**) OXTr-Venus knock-in mice have TH^{+} VTA DA neurons (red) that express OXTr (green) in close proximity to OXT fibers (magenta). Scale bars, 100 μm. (**D**) Diagram of viruses injected into the VTA and PVN of wild-type (WT) mice to silence VTA-projecting PVN neurons. (**E** to **G**) Quantification of social

conditioned place preference (CPP) in mice expressing ZsGreen or Kir2.1 ($n = 8$ for both groups) in VTA-projecting PVN neurons. (**H**) Diagram of Cre virus injection into the VTA of *OXTr*$^{fl/fl}$ or WT mice ($n = 9$ for both groups). (**I** to **K**) Quantification of social CPP in OXTr$^{fl/fl}$ or WTmice receiving VTA virus injections. (**L**) Diagram of genetic cross to delete OXTrs from DA neurons (fig. S3 shows the detailed breeding strategy). (**M** to **O**) Quantification of social CPP in WT ($n = 26$) or homozygous DA OXTr KO ($n = 25$) mice. (**P**) Diagram of genetic cross to delete OXTrs from GAD2-expresing γ-aminobutyric acid (GABA) neurons. (**Q** to **S**) Quantification of social CPP in WT ($n = 27$) or homozygous GABA OXTr KO ($n = 27$) mice. Data shown are means ± SEM. Significance was calculated by means of paired *t* tests for within-group comparisons and unpaired *t* tests for across-group comparisons. *$P < 0.05$; **$P < 0.01$; ***$P < 0.001$; ****$P < 0.0001$. Comparisons with no asterisk were considered not significant (n.s.; $P > 0.05$).

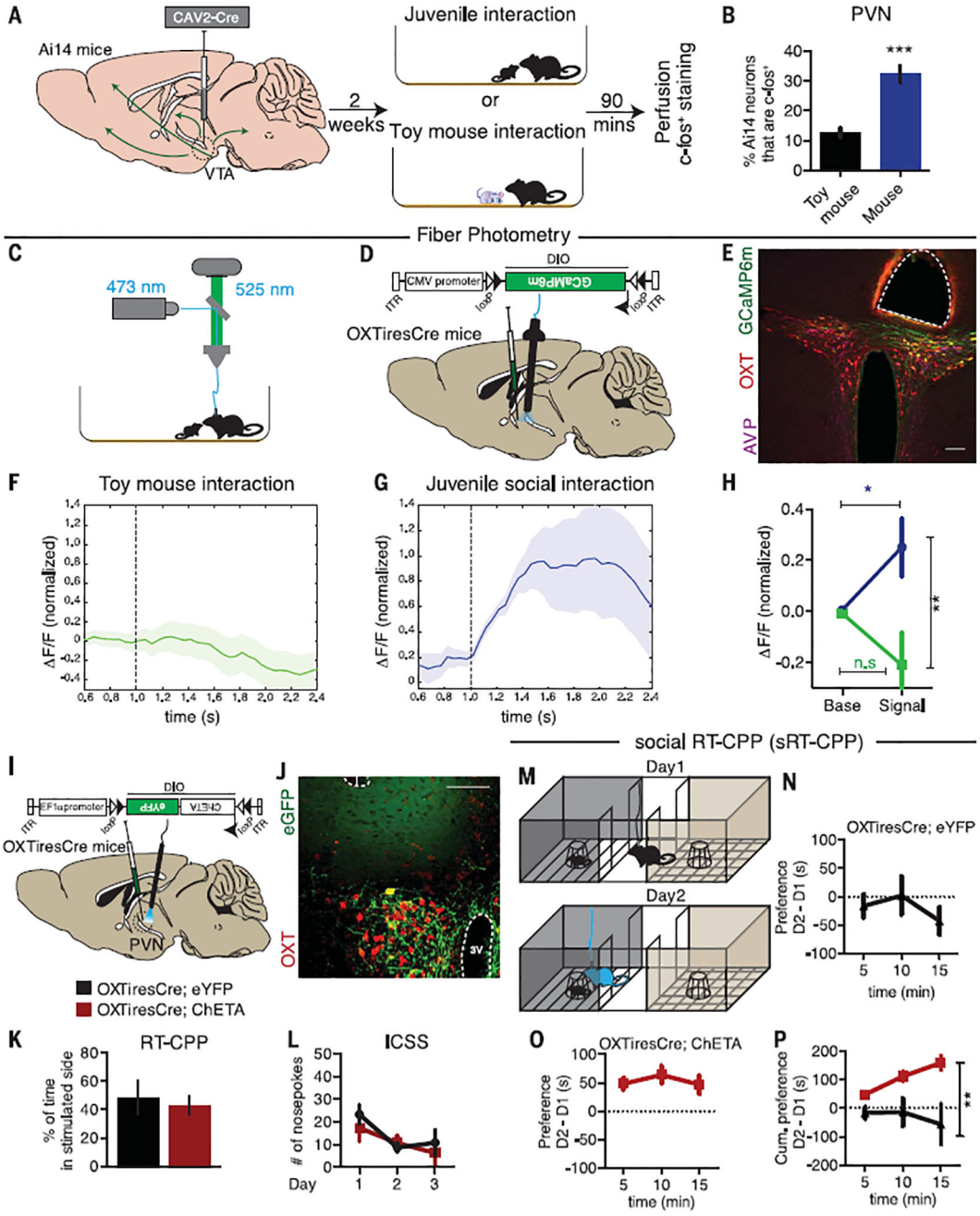

Fig. 2. PVN OXT neuronal activity is enhanced during social interaction and is sufficient to induce social real-time CPP.

(**A**) Ai14 tdTomato reporter mice were injected with CAV2-Cre in the VTA and subjected to interaction with either a juvenile mouse ($n = 5$) or a toy mouse ($n = 3$). (**B**) Quantification of the percentage of tdTomato-positive cells, whichare known to project to the VTA, that were also *c-fos*–positive. (**C** and **D**) Diagrams showing the methods used to record GCaMP6m activity in PVN OXT neurons. (**E**) Immunohistological image showing fiber placement in close proximity to PVN OXT neurons (red) expressing GCaMP6m (green). Scale bar,100 μm. (**F** and **G**) Time course plots showing event-locked average *z*-scores of GCaMP6m

transients in response to social interactions with a toy mouse (n = 16 events from an individual mouse) or with a juvenile mouse (n = 7 events from an individual mouse). Shaded areas, SEM. $\Delta F/F$, normalized change in fluorescence. (**H**) Plot of average fluorescent signal for 1 s beforeand 1 s after the onset of a toy interaction event (n = 26 events from four mice) or juvenile interaction event (n = 25 events from six mice). (**I**) Diagram showing how AAV_{DJ}-DIO-ChETA-eYFP was injected into the PVN of OXTiresCre mice with optical fibers implanted in the PVN. (**J**) Immunohistological images showing fiber placement and colocalization of eGFP (green) and OXT neurons (red) in the PVN. Scale bar, 100 μm. 3V, third ventricle. (**K**) Quantification of real-time CPP (RT-CPP) for eYFP-expressing (black; n = 4) and ChETA-expressing (red; n = 6) mice. (**L**) Operant nose-poking to receive 30-Hz light stimulation did not differ between eYFP- and ChETA-expressing mice (n = 8 for both groups). (**M**) Diagram showing the social RT-CPP (sRT-CPP) protocol. (**N** and **O**) Time spent in social chamber on day 1 (D1) subtracted from time spent on day 2 (D2) for eYFP- and ChETA-expressing mice, graphed in 5-min bins (n = 10 mice in each group). (**P**) Cumulative subtracted preference over the 15-min test period. Data shown are means ± SEM. Significance was calculated by means of unpaired t tests for across-group comparisons in (B), (H), and (K) and two-way analysis of variance (ANOVA) for (P). $*P < 0.05$; $**P < 0.01$; $***P < 0.001$.

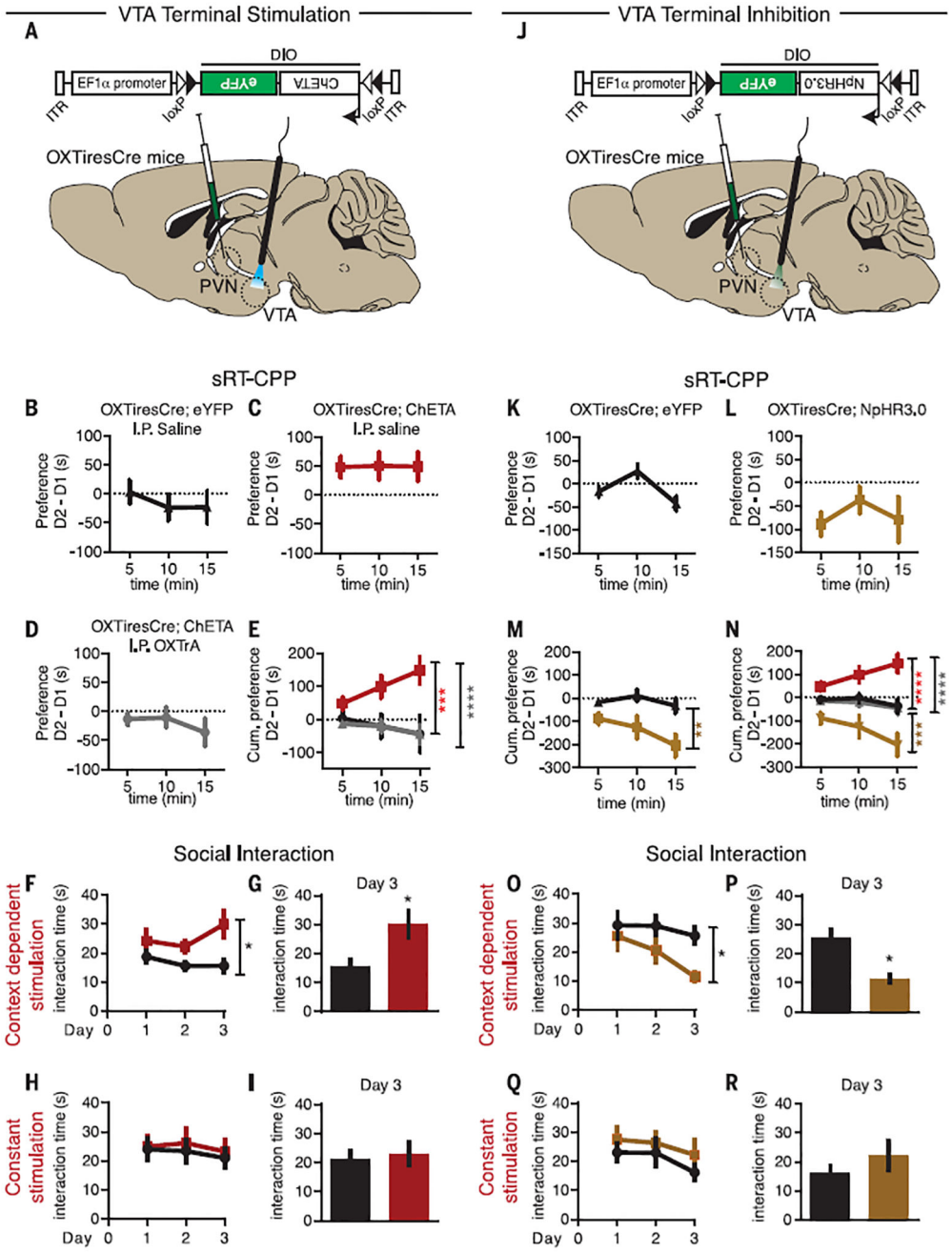

Fig. 3. Bidirectional control of sociability by bidirectional control of OXT release in the VTA.

(**A**) AAV_{DJ}-DIO-ChETA-eYFP was injected into the PVN of OXTiresCre mice with optical fibers implanted in the VTA. (**B** to **D**) Quantification of sRT-CPP (as in Fig. 2) for eYFP-expressing (black; $n = 7$) and ChETA-expressing (red; $n = 12$) mice injected intraperitoneally (I.P.) with saline and ChETA-expressing mice (gray; $n = 12$) injected intraperitoneally with an OXTr antagonist (OXTrA). (**E**) Cumulative subtracted preference over the 15-min test period. (**F** to **I**) Effects of context-dependent [(F) and(G)] versus constant [(H) and (I)] stimulation of OXT fibers in the VTA on time spent interacting during the free juvenile interaction test over 3 days [(F) and (H)] and on day 3 only [(G) and(I)] [*n*

= 18 and 22 mice for the eYFP (black) and ChETA (red) groups, respectively]. (**J**) OXTiresCre mice were injected with AAV_{DJ}-DIO-NpHR3.0-eYFP in the PVN with optical fibers implanted in the VTA. (**K** to **M**) Effects on sRT-CPP of inhibiting OXT fibers in the VTA through NpHR3.0 activation [n = 9 and 11 for the eYFP (black) and NpHR3.0 (yellow) groups, respectively]. (**N**) Summary comparing effects of activating or inhibiting OXT fibers in the VTA, along with control experiments [color-coding as in panels (B) to (M)]. (**O** to **R**) Effects of context-dependent [(O) and (P)] versus constant [(Q) and (R)] inhibition of OXT fibers in the VTA on time spent interacting during the free juvenile interaction test over 3 days [(O) and (Q)] and on day 3 only [(P) and (R)] [n = 16 and 16 for the eYFP (black) and NpHR3.0 (yellow) groups, respectively]. Data shown are means ± SEM. Significance was calculated by means of unpaired t tests for across-group comparisons in (G), (I), (P), and (R) and two-way ANOVA for (E), (F), (H), (M), (N), (O), and (Q), with Bonferroni's multiple comparison post-hoc test for (E), (M), and (N). *P < 0.05; **P < 0.01; ***P < 0.001; ****P < 0.0001.

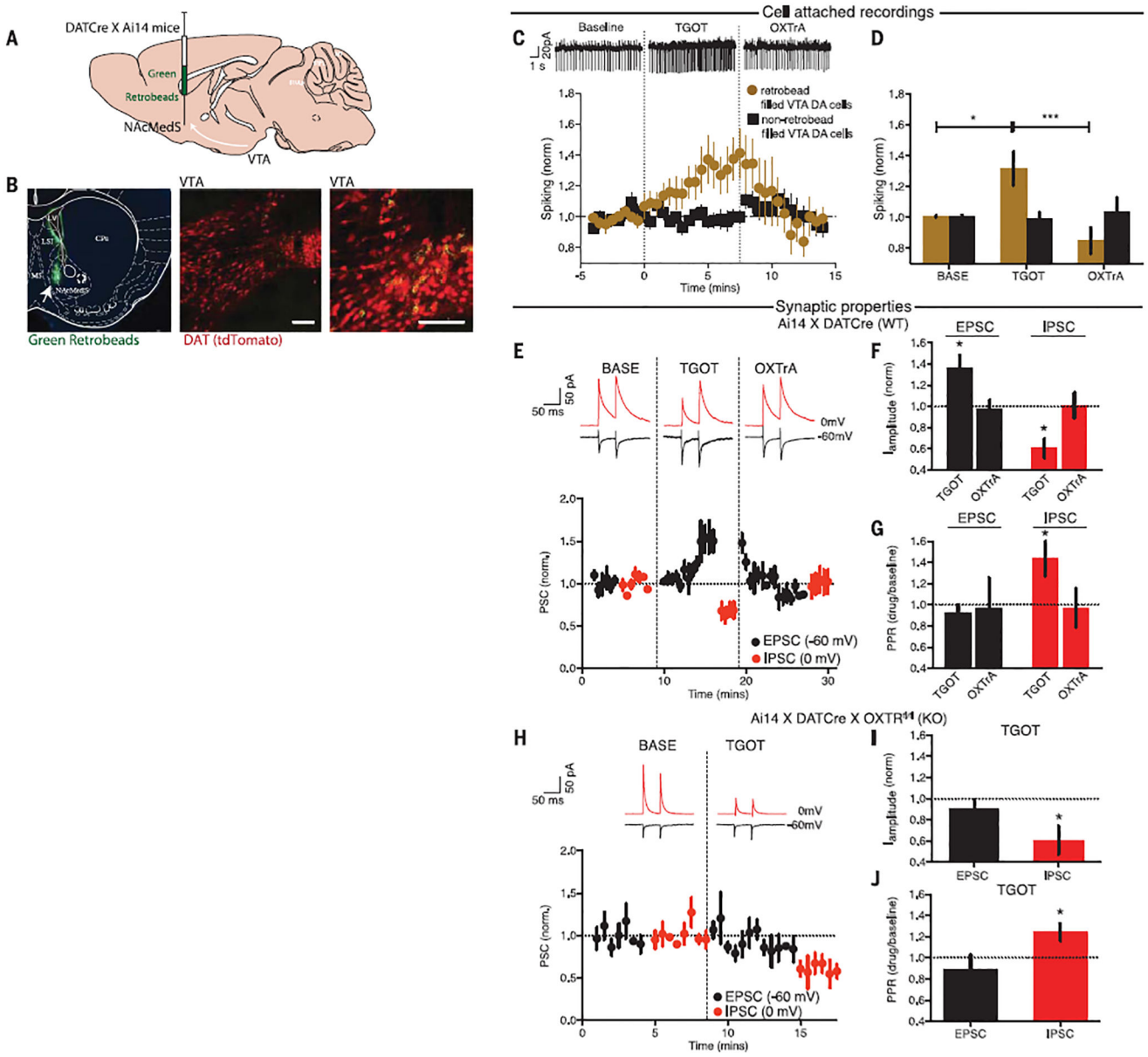

Fig. 4. OXT increases the excitation-to-inhibition balance in NAcMedS-projecting VTA DA cells.

(**A**) Green retrobeads were injected into the NAcMedS of Ai14:DATCre mice to label DA neurons. (**B**) Coronal section of NAc showing the injection site (left), tdTomato-containing VTA DA cells (middle), and a higher magnification of retrobead-containing VTA DA cells (right). Scale bars, 100 μm. (**C**) Sample traces of spiking in retrobead-filled VTA DA cells (top) and time course (bottom) of the effect of TGOT and OXTrA on spontaneous spiking of VTA DA cells for both retrobead-filled (yellow; $n = 10$) and nonfilled (black; $n = 8$) cells. (**D**) Quantification of spiking (BASE, baseline). (**E**) Sample traces (top) and time course (bottom) of the amplitude of evoked EPSCs (black) and IPSCs (red) in VTA DA cells projecting to NAcMedS during TGOT application and after its washout with application of OXTrA ($n = 11$ cells). (**F**) Summary of EPSC and IPSC changes. *I*, current. (**G**) Summary of changes in paired pulse ratios (PPRs). (**H**) Sample traces (top) and time course (bottom) of

the amplitudes of EPSCs and IPSCs in VTA DA cells projecting to NAcMedS during TGOT application in slices from mice lacking OXTrs in DA cells ($n = 4$ cells). (**I**) Summary of EPSC and IPSC changes. (**J**) Summary of changes in paired pulse ratios. Data shown are means ± SEM. Significance was calculated by means of unpaired *t* tests for comparisons with baseline in (F), (G),(I), and (J) and one-way ANOVA with Bonferroni's multiple comparison post-hoc test for (D). *P < 0.05; ***P < 0.001.